

Competitive effect of calcium lactate and epoxidized soil bean oil on crystallization kinetics of polypropylene

Buncha Suksut*, Chonticha Seesong, Nutchalida Phueaksri, Chantarawan Chuephlob

Faculty of Engineering and Technology, King Mongkuk's University of Technology North Bangkok, Rayong Campus, Rayong 21120, Thailand

Received: 27 September 2023, Accepted: 6 November 2023

ABSTRACT

The effect of calcium lactate (CL) and epoxidized soil bean (ESO) on the crystallization kinetics of polypropylene (PP) was investigated by using polarized optical microscopy (POM) and differential scanning calorimetry (DSC) techniques. The experiments were performed under both non-isothermal and isothermal conditions. The development of spherulitic microstructure and crystallization kinetics were influenced by both CL and ESO. CL is an efficient nucleating agent for the crystallization of PP. The addition of CL facilitated faster spherulite growth and crystallization rate, while reduced the spherulite size. An opposite performance was discovered with the incorporation of ESO. Nucleation effect of CL on the PP crystallization was less effective with the presence of ESO. Compared with PP/CL, PP/CL/ESO provided a large spherulite size, slow spherulite growth, and a low crystallization rate. This is attributed to the ESO inhibiting the nucleation site of CL. However, the degree of crystallinity and the Avrami exponents remained unchanged with the inclusion of both CL and ESO. **Polyolefins J (2024) 11: 29-41**

Keywords: Crystallization kinetic; calcium lactate; epoxidized soil bean; polypropylene; spherulite.

INTRODUCTION

As is known, the thermoplastic performance is strongly governed by microstructure of semicrystalline polymer. During the solidification of the melt, semicrystalline polymer can be crystallized. There are two main steps of crystallization process: nucleation and crystal growth. When the crystallization is completed, there is a full of spherulites in the entire volume of material [1]. The spherulitic structures are discontinuities that can change the properties of the semicrystalline polymer. Therefore, understanding of the crystallization

kinetics is very crucial and advantageous to forecast the most relevant manufacturing conditions and to correlate the microstructure development with the kinetics of crystallization [2]. The kinetics of quiescent crystallization are commonly analyzed under isothermal or non-isothermal circumstances. This study can help to clarify the crystallization mechanism, which is crucial for optimizing the polymer processing and understanding the process-structure-property relationship. The kinetics of isothermal crystallization

*Corresponding Author - E-mail: buncha.s@eat.kmutnb.ac.th

is generally investigated using data received from exothermic peaks in the DSC thermogram. This kinetic is based on the hypothesis that the heat derived during the evolution of crystallization directly corresponds to the progress of crystallinity [3].

For polymer composites, this circumstance is more complex. The existence of fillers can alter the microstructure of the matrix that acts as a nucleating agent. The nucleus size needed for crystal growth can be reduced by a foreign surface. The formation of the interface between polymer crystal and foreign particle is less obstructed than the formation of the corresponding free polymer crystal surfaces. Therefore, the free energy opposing primary nucleation is reduced by a foreign pre-existing surface of heterogeneous nucleation [4]. As a result, the value of the fold surface free energy is reduced, thereby giving rise to an increase in crystallization rate. However, this situation is further complicated by ternary compositions. Previous studies attempted to analyze the combined effect of fillers and plasticizers on polymer matrix crystallization. This is often found that the crystallization can be influenced by the nucleation effect of fillers, and by retarding effect of plasticizers [5-6].

Polypropylene (PP) is a commodity thermoplastic polymer and widely used in many industries. This is because of its outstanding properties, low cost, and easy processability. However, as compared to engineering plastics, the application of PP is still limited by its low stiffness. To improve the performance of PP, the incorporation of filler is one of the most successful techniques. Fillers usually impact the ultimate performance in two approaches: by acting as reinforcement agents and affecting the crystallization of the polymer matrix [7]. Several fillers, such as calcium carbonate (CaCO_3) [8], silica dioxide (SiO_2) [7], titanium dioxide (TiO_2) [9], multi-walled carbon nanotubes (MWCNTs) [10], microcrystalline cellulose (MCC) [11], and biochar (BC) [12] have been incorporated into PP to improve its performance. Recently, calcium lactate (CL), bio-based renewable filler, has been considered a great filler option because of its renewable material and biocompatibility [13]. In our previous work, the results revealed that CL particles can improve the mechanical properties of PP [14]. We were also able to show that CL changed the crystallization behavior of PP. The CL provided faster crystallization and a small spherulite size.

However, the reinforcement effect of CL accompanies by a decrease in the flexibility of PP. To balance between the stiffness and flexibility, epoxidized soybean

oil (ESO) was added as plasticizer deriving from renewable plants. Because of growing environmental awareness, the use of CL as bio-filler, and ESO as bio-plasticizer for PP matrix is of our interest. Objective of this research work is to elucidate the effect of CL and ESO on the kinetics of PP crystallization under both non-isothermal and isothermal conditions. All experiments were performed using both microscopy and calorimetry techniques.

EXPERIMENTAL

Materials

A commercial grade polypropylene (PP) (HP553R) was purchased from HMC Polymer Co., Ltd. and calcium lactate (CL) was purchased from PURAC (Thailand) Ltd. The morphology of the CL particle was revealed by the high-resolution SEM image. Epoxidized soil bean (ESO) was supplied by Srithepthai Chemical Co. Ltd., and used as plasticizer.

Preparation of composites

From our previous work [14], the CL content of 40 wt.% provided the optimum properties of PP/CL composites and was chosen to be used in this study. The neat PP and PP filled with 40 wt.% of CL were compounded in an internal mixer (MX500, Chareon Tut) followed by a co-rotating twin screw extruder (CTED22L32, Chareon Tut). The PP/CL composite was blended with 3 phr of ESO. Injection molding (60SE, JONWAI) was used to prepare the testing samples.

Fourier transform infrared spectroscopy (FTIR)

The interaction between the PP, CL, and ESO was monitored by a FTIR (Frontier, Perkin-Elmer). Thin films of about 20 μm were sectioned from the bulk samples using a steel knife of rotation microtome (Hyrax M 25, Carl Zeiss MicroImaging GmbH). The spectra in the range of 4000-500 cm^{-1} were used.

Scanning electron microscopy (SEM)

The fractured surface morphology of PP and its composites was analyzed by the SEM (Prisma E, Thermo Scientific) at room temperature. Prior to the measurement, the fractured surface was coated with gold for 90 seconds. An acceleration voltage of 20 kV was used to record the SEM images for the sample.

Polarized optical microscopy (POM)

In order to study the crystallization, thin sections

of about 10 μm were sliced from the center of the rectangular bars using a steel knife of rotation microtome (Hyrax M 25, Carl Zeiss MicroImaging GmbH, Jena, Germany). The samples were prepared by placing a thin section of 10 μm on a glass slide and placing a cover slip on top of the thin section. The growth of PP spherulite was performed under both non-isothermal and isothermal conditions by using a transmitted-light microscope (DM2700M, Leica) equipped with a heating stage (LTS420, LINKAM). For non-isothermal experiments, the thin section was heated with a heating rate of 20°C/min to 210°C and kept for 5 minutes at 210°C to eliminate the previous processing history. It was then cooled to room temperature with different cooling rates (5, 10, 15 and 20°C/min). When performing isothermal experiments, the samples were cooled at a rate of 40°C/min to various chosen temperatures (125°C, 130°C, 135°C, 140°C) and kept constant at those temperatures until an impingement of spherulite was fully completed.

Differential scanning calorimetry (DSC)

The thermal analyses were figured out using a differential scanning calorimeter (DSC, Q200, TA instruments) connected with a Refrigerated Cooling Systems 90 (RCS90). To calibrate the melting enthalpy and the temperature scale, the indium was chosen as a reference material. The weight of each sample was approximately between 5 and 10 mg. The samples were placed in the Tzero pan and completely closed with a lid.

For non-isothermal crystallization, the sample was initially heated from 0°C to 210°C at a rate of 20°C/min under nitrogen atmosphere and remained for 5 min at 210°C to destroy previous process history. Subsequently, the sample was cooled to 0°C at different cooling rates (5, 10, 15, and 20°C/min). The crystallization temperature peak during cooling (T_c) was detected. The degree of crystallinity (X_c) was determined as:

$$\%X_c = \frac{\Delta H_m}{(1-\phi)\Delta H_m^o} \times 100$$

where ΔH_m is the enthalpy of melting, ΔH_m^o is the theoretical heat of fusion for 100% crystalline PP, and ϕ is the weight fraction of filler in the composite (209 J/g) [15].

In order to obtain crystallization kinetic information, an isothermal crystallization experiment was measured at different crystallization temperatures. Based on the

non-isothermal experiment results, four temperatures with a step of 5°C were decided as the isothermal crystallization temperature (125, 130, 135, and 140°C). The samples were quenched at a rate of 40 K/min to certain isothermal crystallization temperatures (T_i), and stay constant at that temperature until complete crystallization.

The isothermal crystallization kinetic can be interpreted based on the Avrami equation [16]:

$$X_t = 1 - \exp(-Kt^n)$$

where K is the constant of crystallization rate which is referred to the nucleation and growth rates. n is the Avrami exponent involving the mechanism of nucleation and the geometry of growth. The values of K and n can be obtained by fitting the experimental data of X_t versus t using the double logarithmic form of equation:

$$\log[-\ln(1 - X_t)] = \log K + n \log t$$

Lorenzo et al. [17] modified an equation that combines the induction time, t_0 . For DSC measurement, the t_0 is the time at isothermal crystallization temperature that could elapse before crystallization begins [18]. By applying the t_0 , the kinetic expression is as follows:

$$\log[-\ln(1 - X_t)] = \log K + n \log(t - t_0)$$

The $t_{1/2}$ is the half time of crystallization which defined as the time needed to reach a half of complete crystallization process and can be expressed as:

$$t_{1/2,iso} = (\ln 2/K)^{1/n}$$

RESULTS AND DISCUSSION

Structure analysis by FTIR

The infrared spectrum of all samples in the range of 500-4000 cm^{-1} is presented in Figure 1. For neat PP, the stretching vibration mode of the C-CH₃ bond is exhibited at an absorption peak of 840 cm^{-1} . The rocking vibration mode of the -CH₃ group is detected at absorption peaks of 972, 997, and 1165 cm^{-1} . The absorption peak located at 1375 cm^{-1} is assigned to -CH₃ symmetric bending vibration. The absorption peak at 2952 cm^{-1} corresponds to the asymmetric stretching vibration mode of the -CH₃ group. All the previously mentioned absorption peaks are associated

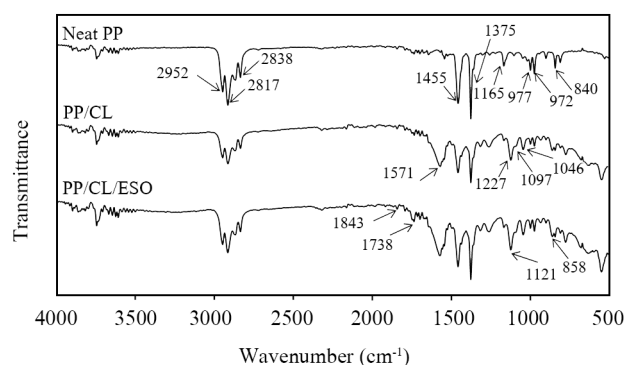


Figure 1. FTIR spectra of neat PP, PP/CL and PP/CL/ESO composites. Arrows indicate the specific wavenumber.

with the methyl group in the PP [19]. The spectrum of neat PP also reveals prominent peaks, including 1455, 2838, and 2917 cm^{-1} , representing $-\text{CH}_2-$ symmetric bending, $-\text{CH}_2-$ symmetric stretching, and $-\text{CH}_2-$ asymmetric stretching, respectively [19]. The FTIR spectrum of PP/CL shows absorption peaks near 1127, 1097, and 1046 cm^{-1} corresponding vibration of various C-O bonds, and at 1571 cm^{-1} indicating to the

carboxylate (COO^-) groups [20-21], which represents the characteristic of CL. The FTIR spectrum of PP/CL/ESO exposes an absorption peak of C=O stretching of the ester group around 1738 cm^{-1} , and a C-O-C asymmetric stretching vibration of the epoxy group. Characteristic peaks of ester and epoxy groups confirm the principle functional group of ESO [22-25]. The results show that there is no occurrence of any new significant absorption peak due to the presence of CL and ESO in the PP matrix. This suggests the absence of any strong chemical interaction in the composite samples [20, 26].

Fractured surface measurement by SEM

In general, the filler dispersion and the interfacial interaction between filler and polymer matrix determine the properties of the composites [12]. The morphological feature of CL is revealed in Figure 2 (a). A particulate form with an estimated size in the range of 100-200 μm is detected. SEM images of the fractured surfaces of neat PP, PP/CL, and PP/CL/ESO are also shown in Figure 2. For neat PP, a homogeneous and

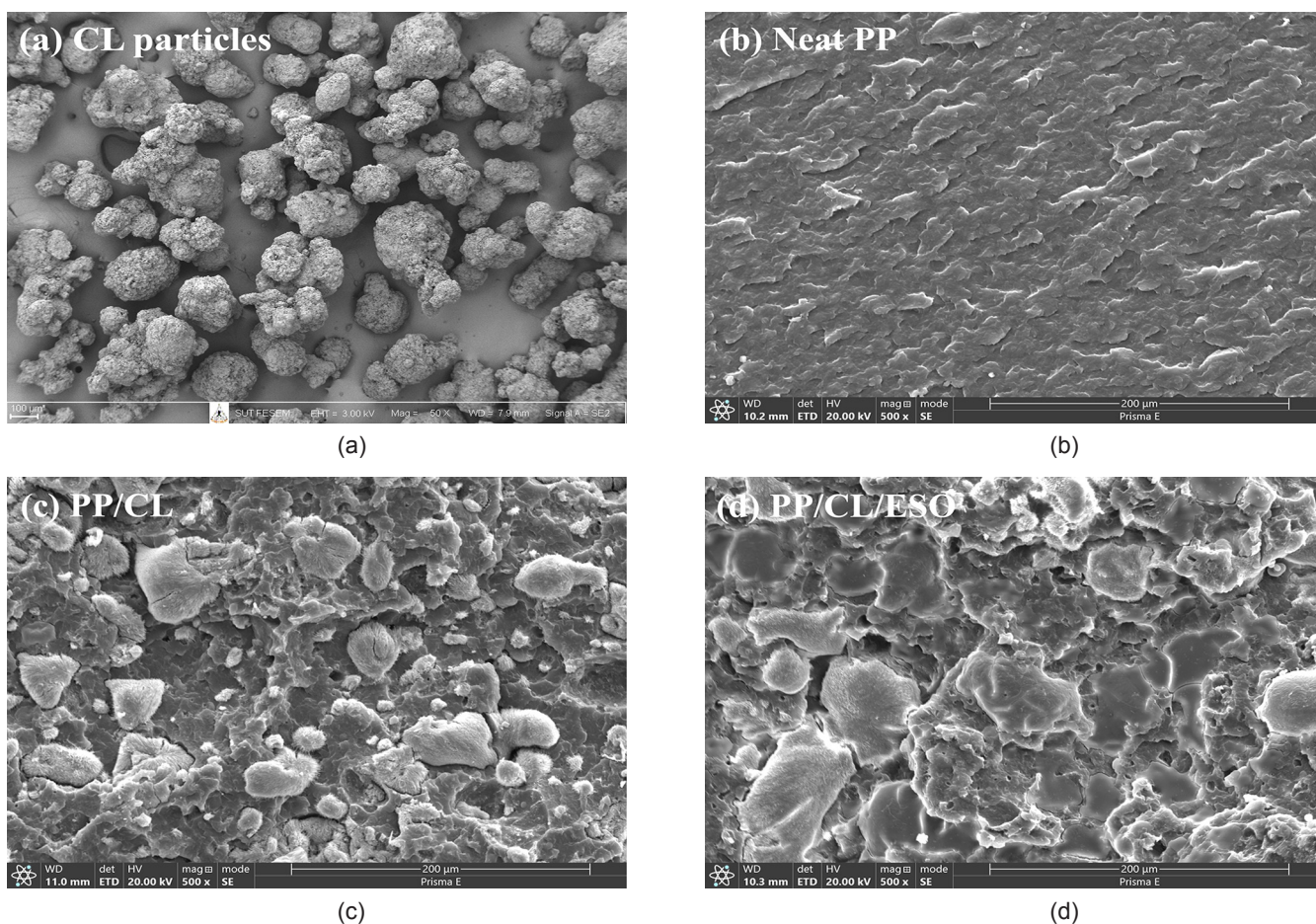


Figure 2. SEM micrographs of (a) CL particles, (b) fractured surface of neat PP, (c) fractured surface of PP/CL, and (d) fractured surface of PP/CL/ESO.

flat surface is observed, as presented in Figure 2 (b). In Figure 2 (c), the SEM image shows the existence of CL particles as dispersed phase. Although CL particles are quite evenly dispersed in the PP matrix, the formation of agglomeration can be found in some areas on the PP surface. Furthermore, some of the CL particles are embedded in the PP matrix, as shown in Figure 2 (d). It suggests good adhesion between the CL and PP, which is influenced by the presence of ESO [11]. From the FTIR and SEM results, it can be deduced that there is no chemical interaction between CL and PP; the improved adhesion between both materials may be due to physical interaction as a consequence of ESO's existence.

Non-isothermal crystallization by POM

Figure 3 presents the evolution of the spherulitic microstructure of samples under polarized optical microscope at different cooling rates. The images are captured during cooling at certain temperatures (145°C and 130°C). At 145°C, neat PP shows an almost clear molten PP, and a few tiny spherulites are detected. Maltase cross pattern of regular spherulite

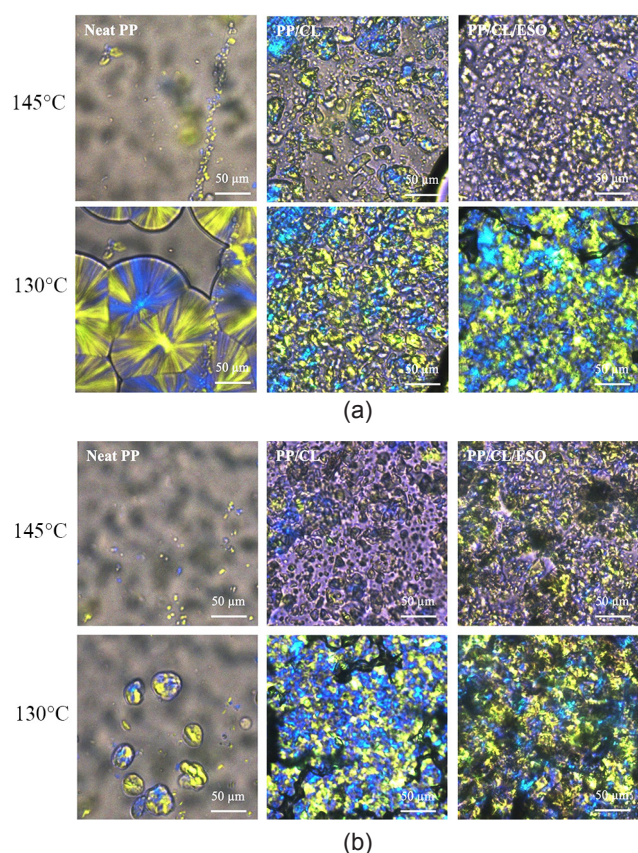


Figure 3. Spherulitic development of neat PP and its composites recorded from non-isothermal crystallization during the first cooling process captured at 145°C and 130°C and at different cooling rates of (a) 5°C/min, and (b) 10°C/min.

is observed for neat PP. Although the spherulites are noticeable in the PP/CL and PP/CL/ESO composites, there are irregular spherulitic grains without Maltese cross pattern [7]. It is clear that CL particles contribute to the faster crystallization of PP. However, the effect of ESO on the spherulite development of PP during cooling conditions is not obvious in this study. Moreover, it can be found that as the cooling rate increases, a smaller spherulite size appears at the given temperature. For the high cooling rates, the lower temperatures favor nuclei formation, producing a higher density of spherulites site and thus smaller sizes of spherulite [27]. The spherulites continue to grow in all samples at a temperature of 130°C.

Isothermal crystallization by POM

Figure 4 displays the optical micrographs of neat PP, PP/CL, and PP/CL/ESO captured in isothermal conditions. The density of spherulites site depends on the crystallization temperature. The number of spherulites in neat PP decreases as crystallization temperature increases. This is because the creation of nuclei depends on the degree of supercooling [27]. At

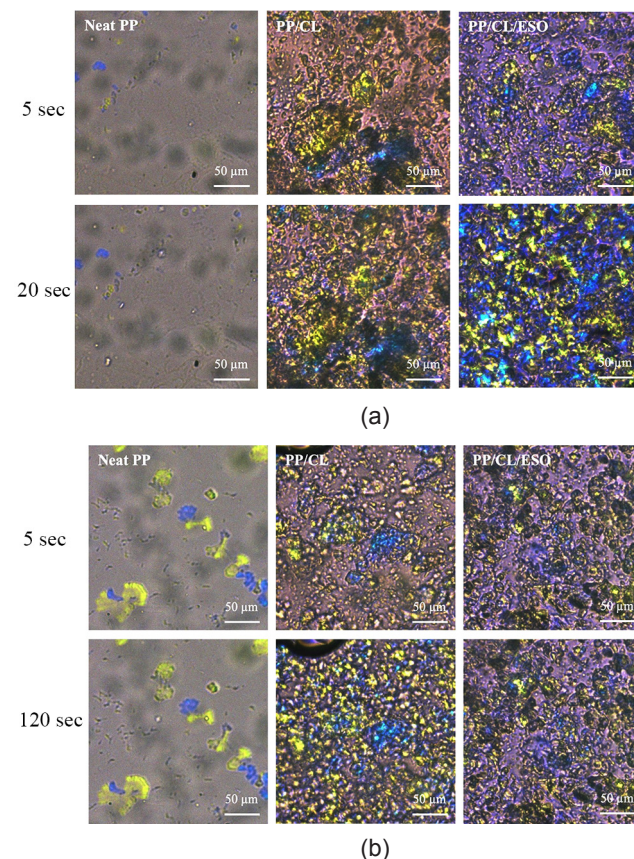


Figure 4. Spherulitic development of neat PP and its composites obtained from isothermal crystallization at different temperatures: (a) 130°C and (b) 140°C.

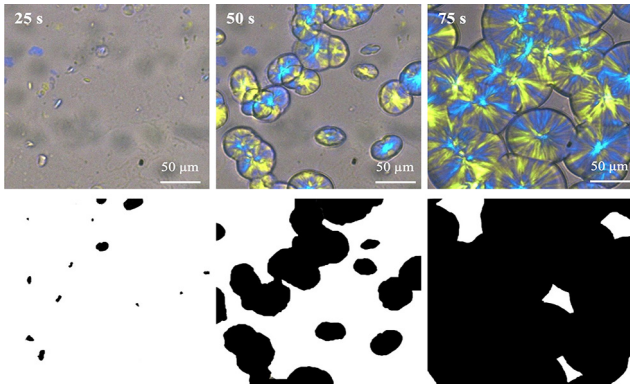


Figure 5. Spherulitic development of neat PP as a function of times during isothermal crystallization at 130°C: Original optical micrographs (top), greyscale images after processing with Photoshop (bottom).

a high degree of supercooling (lower crystallization temperature), a large amount of spherulites of neat PP is detected. In the opposite way, a small number of spherulites is attained when the degree of supercooling is reduced (high crystallization temperature). Furthermore, the presence of CL particles forms higher nucleation sites, resulting in smaller spherulites as compared to neat PP. As expected, the spherulite size of PP in the PP/CL/ESO composite seems to be larger than that of PP/CL. This means that the

addition of ESO to the PP/CL composite hinders the chain mobility, therefore the nucleation effect of CL particles.

As shown in Figure 5, the development of spherulite is a function of isothermal crystallization time. The optical micrographs were converted to greyscale images, and then the spherulite growth area was calculated in Photoshop. A plot of the spherulite growth area and time of all samples is exhibited in Figure 6. At certain temperatures, it is obvious that in the case of neat PP, the spherulites require a very long period to reach their ultimate area of growth. In the case of PP/CL and PP/CL/ESO, the beginning of the spherulite growth is not possible to capture due to the very fast crystallization of both materials. Moreover, the presence of CL particles shortens the completion time of spherulite growth. However, the completion of spherulite growth of PP/CL/ESO is faster than that of neat PP but slower than that of PP/CL. This is evidence of the competitive effect between CL and ESO on the spherulite growth of PP. For all samples, it is also observed from Figure 6 that spherulite growth decreases when crystallization temperature increases. At a higher crystallization temperature, the spherulite growth takes more time to complete.

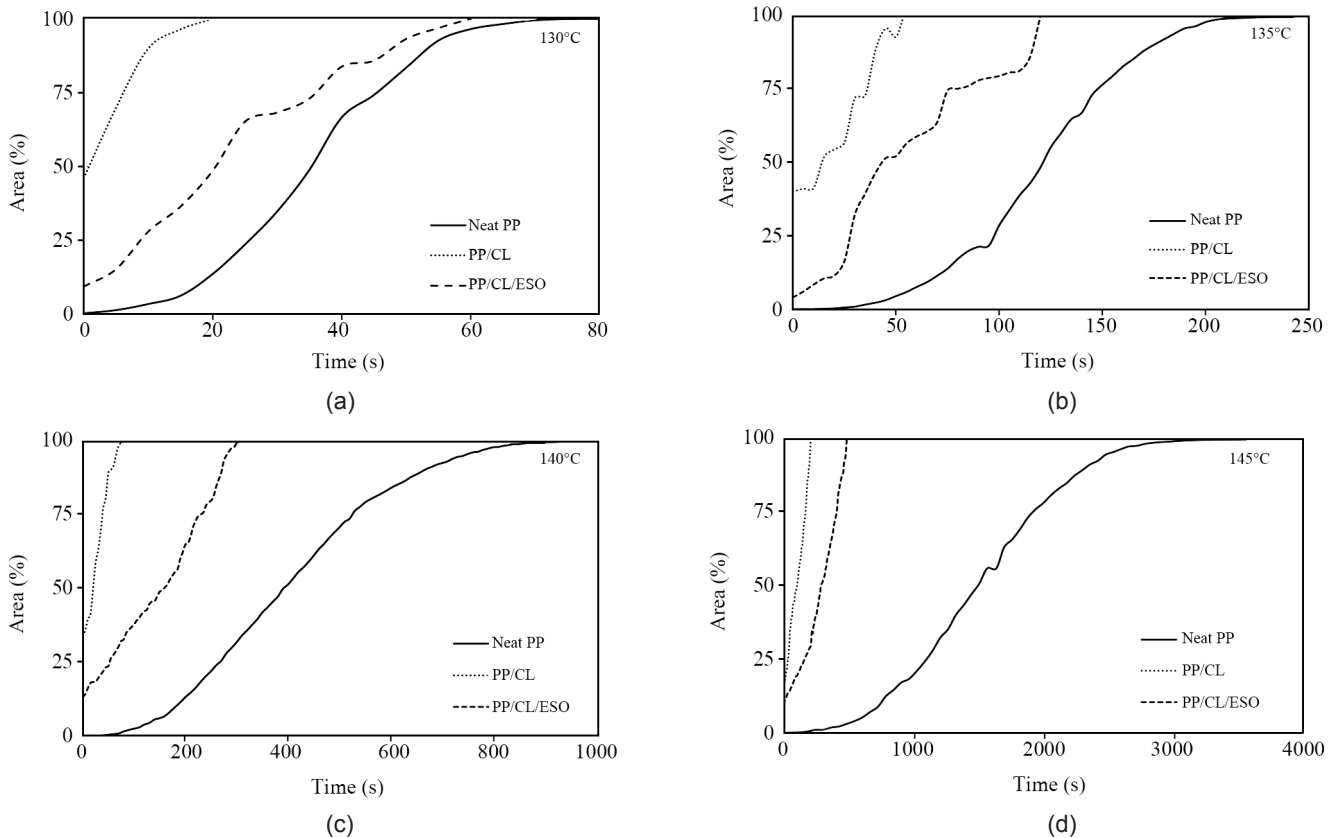


Figure 6. Spherulite growth of neat PP and its composites versus time during various isothermal crystallization temperatures.

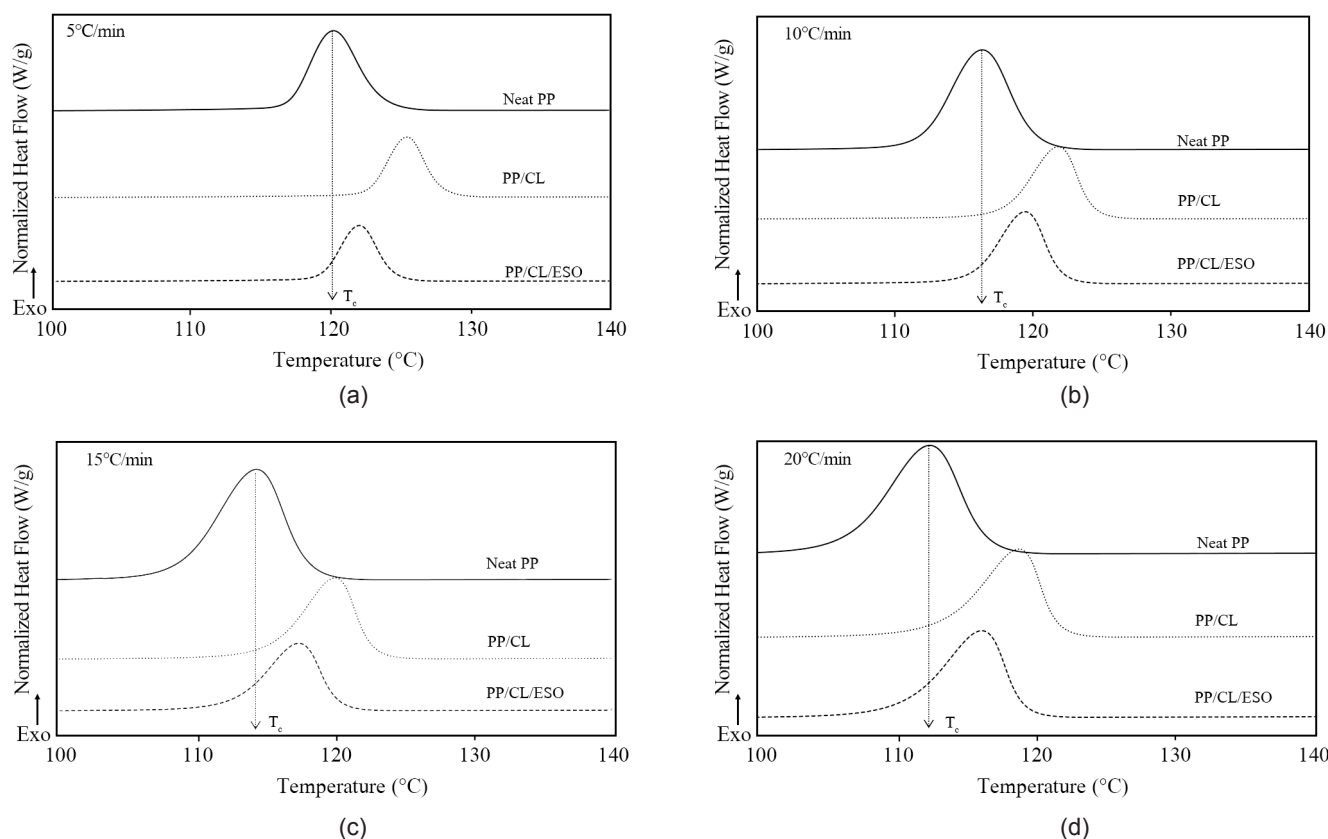


Figure 7. Non-isothermal DSC thermograms of neat PP and its composites during the first cooling process at different cooling rates of: (a) 5°C/min, (b) 10°C/min, (c) 15°C/min, and (d) 20°C/min.

Non-isothermal crystallization by DSC

Figure 7 presents the non-isothermal crystallization exothermic thermograms of neat PP and its composites with different cooling rates. The values of non-isothermal crystallization peak T_c , melt temperature peak (T_m), and degree of crystallinity (X_c) are listed in Table 1. For all cooling rates, T_c shifts to higher temperature by incorporation of CL. It means that the presence of CL initiates faster crystallization,

Table 1. DSC non-isothermal crystallization results of neat PP and its composites at different cooling rates

| Samples | Cooling rates (°C/min) | T_c (°C) | T_m (°C) | X_c (%) | $t_{1/2,iso}$ (min) |
|-----------|------------------------|------------|------------|-----------|---------------------|
| Neat PP | 5 | 120.1 | 160.1 | 43.4 | 1.3 |
| | 10 | 116.3 | 160.6 | 42.7 | 0.7 |
| | 15 | 114.4 | 159.8 | 42.2 | 0.6 |
| | 20 | 112.4 | 159.2 | 36.4 | 0.5 |
| PP/CL | 5 | 125.4 | 163.2 | 46.4 | 0.9 |
| | 10 | 121.8 | 162.9 | 47.3 | 0.5 |
| | 15 | 120.1 | 162.2 | 49.2 | 0.4 |
| | 20 | 118.8 | 159.2 | 41.1 | 0.3 |
| PP/CL/ESO | 5 | 121.9 | 162.5 | 38.9 | 1.0 |
| | 10 | 119.4 | 161.7 | 46.4 | 0.6 |
| | 15 | 117.5 | 161.2 | 40.7 | 0.4 |
| | 20 | 116.6 | 160.8 | 40.7 | 0.3 |

independent of cooling rate. However, the retarding effect of ESO on the crystallization of PP is evident. In addition, the crystallization of PP is also affected by cooling rate. For all samples, when the cooling rate increases, the T_c moves to a lower temperature. It implies that at higher cooling rate, the motion of the polymer molecule is slower than the cooling rate, therefore the crystallization initiates at a lower temperature [2]. In addition, the measurement also indicates that the values of T_m and X_c depend on the cooling rate. The presence of CL and ESO has no significant impact on both T_m and X_c of PP.

To evaluate the non-isothermal crystallization rate, the relative crystallinity as a function of temperature ($X(T)$) can be obtained from the below equation [28]:

$$X(T) = \int_{T_0}^T \left(\frac{dH_c}{dT} dT \right) / \int_{T_0}^{T_\infty} \left(\frac{dH_c}{dT} \right) dT$$

where T_0 and T_∞ are the onset and the end of crystallization temperatures, respectively. T is a

temperature at crystallization time, t , and $\frac{dH_c}{dT}$ is the heat flow rate. Crystallization time, t , can be calculated from the following equation:

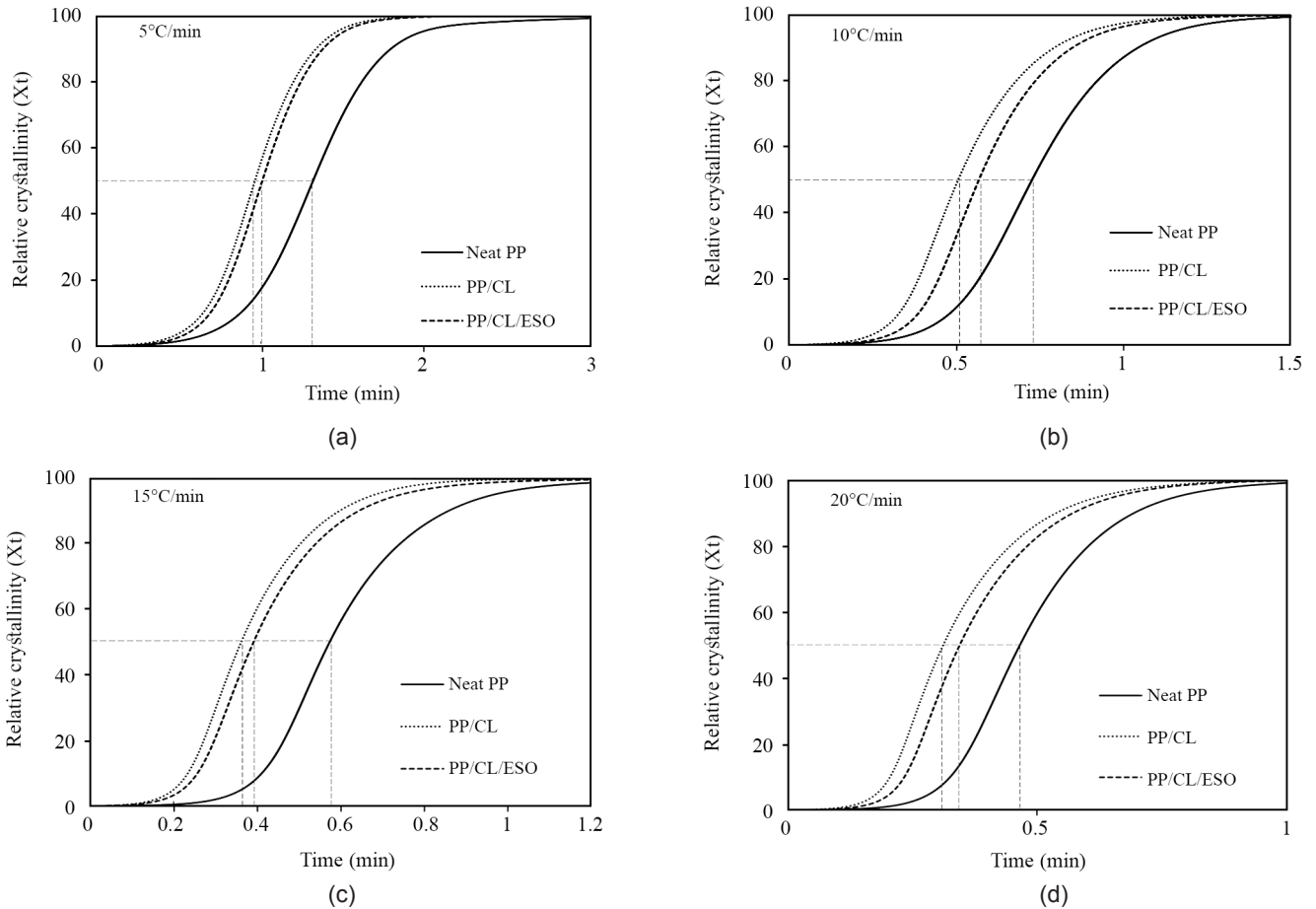


Figure 8. Relative crystallinity as a function of crystallization time of neat PP and its composites at different cooling rates of: (a) 5°C/min, (b) 10°C/min, (c) 15°C/min, and (d) 20°C/min.

$$t = (T_0 - T) / \beta$$

where β is the cooling rate. Thus, the relative crystallinity as a function of time ($X(t)$) can be described as:

$$X(t) = \int_{t_0}^t \left(\frac{dH_c}{dt} dt \right) / \int_{t_0}^{t_\infty} \left(\frac{dH_c}{dt} dt \right)$$

Furthermore, the crystallization half-time $t_{1/2,non}$ can be acquired from the $X(t)$ versus t plots as represented in Figure 8 and Table 1. It is worth to note that the crystallization rate can be considered proportional to the reciprocal half-time of crystallization, $1/t_{1/2,non}$. For all samples, the higher the cooling rate, the shorter the time required for the crystallization process. The presence of CL in the PP composite promotes a faster crystallization rate. On the other hand, the addition of ESO to the PP/CL composite retards the crystallization rate of PP. This is in well agreement with the results obtained from polarized optical micrographs. However, it seems that either CL or ESO do not significantly affect the crystallization rate of PP, as presented in Table 1.

Isothermal crystallization by DSC

To elucidate the effect of CL and ESO on isothermal crystallization of PP, an overlay of DSC exothermic thermograms of all samples at the same temperature is plotted as shown in Figure 9. The results reveal acceleration of crystallization with addition of CL, regardless of crystallization temperature. For neat PP, DSC thermogram exhibits a broad and weak exothermic peak. This implies that it takes a long time to reach the entire crystallization process. In the case of the PP/CL composite, the DSC thermogram shows a sharp and strong exothermic peak. It means that the presence of CL helps to shorten the time to complete crystallization, suggesting that CL has a significant heterogeneous nucleation effect on the PP crystallization, irrespective of the crystallization temperature. As is known, neat polymer is homogeneous nucleation. The formation of homogeneous nucleation is greatly affected by temperature. At high temperatures near the crystal melting point, the crystal nucleus of neat PP is quite difficult to form. While the PP/CL composite is heterogeneous nucleation, and its nucleation is less

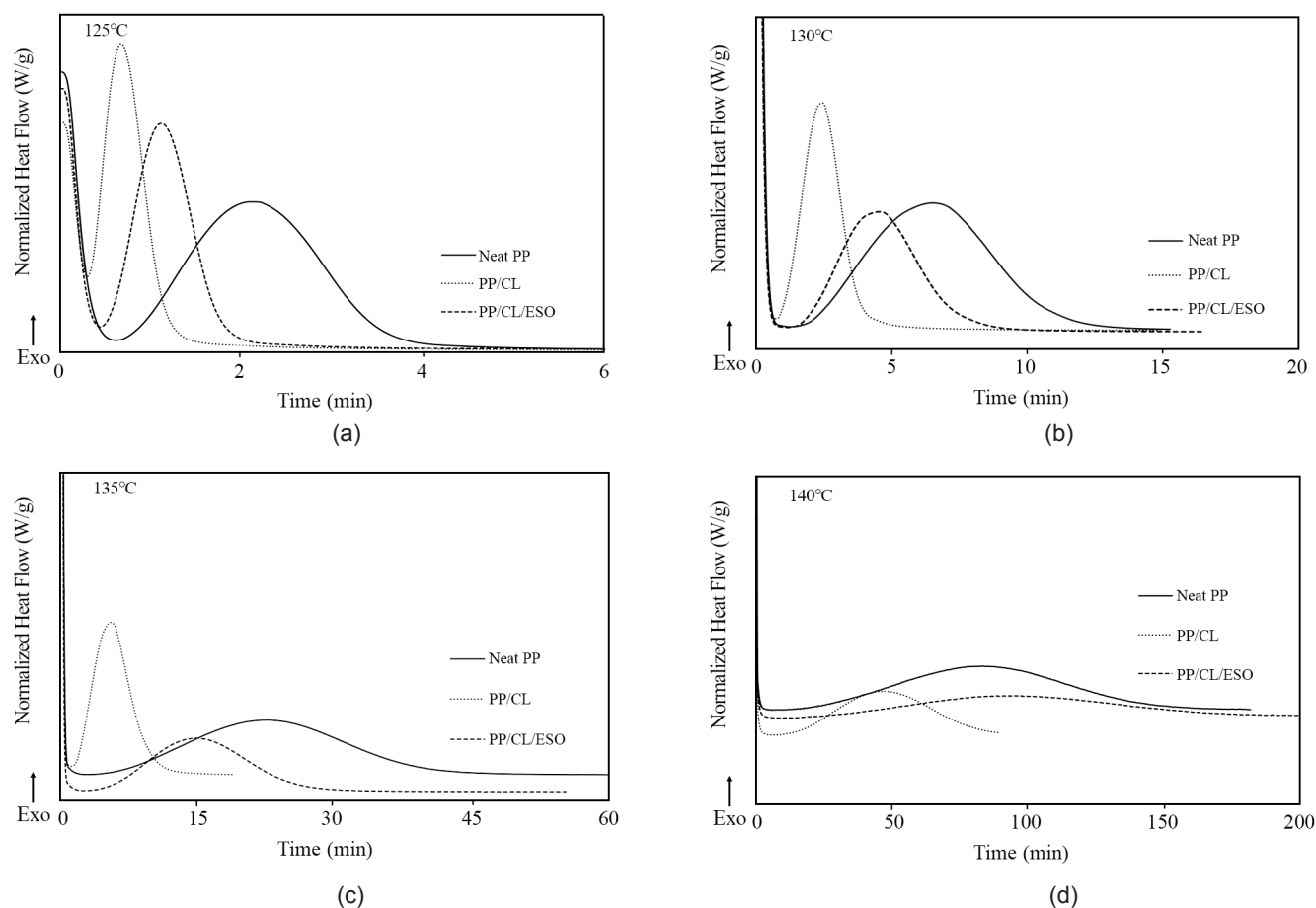


Figure 9. DSC thermograms of neat PP and its composites obtained from isothermal crystallization at different temperatures of: (a) 125°C, (b) 130°C, (c) 135°C, and (d) 140°C.

affected by temperature [29]. Besides, with the addition of ESO to the PP/CL composite, the crystallization peak becomes broader as compared to the binary PP/CL composite. On the contrary, the crystallization peak of the PP/CL/ESO is narrower than that of the neat PP. This result reveals the competitive effect between CL and ESO on the crystallization of PP.

It can be also seen that the required time for crystallization completion of all samples increases when the crystallization temperature increases. For instance, the time of crystallization peak of neat PP is about 2.5 min at the crystallization temperature of 125°C. It is around 90 min when the crystallization temperature reaches 140°C. The same phenomenon was found in both PP/CL and PP/CL/ESO composites. When the crystallization temperature varies from 125°C to 140°C, the time of crystallization peak increases from 0.5 min to 50 min for PP/CL and 1 min to 90 min for PP/CL/ESO. As is known, crystallization process is controlled by the superposition of the crystalline nucleation and growth rate. The crystallization process starts with

the nucleation which is dependence of crystallization temperature. Normally, nucleation is faster at low crystallization temperature as the thermodynamic driving force increases. Therefore, the nucleation is slower at high crystallization temperature, leading to slower crystallization [30].

Figure 10 shows the relative crystallinity as a function of crystallization time of PP and its composites at four different temperatures. It is obvious that all these curves exhibit a similar S-shape. In the early and late stages of crystallization, the growth is very slow but greatly rapid in the middle stage of crystallization. Meanwhile, the S-shape curve shifts to the left side along the crystallization time axis as the presence of CL. This indicates that the time required to complete the crystallization process is shorter as compared to neat PP. For instance, the incorporation of CL facilitates the completion of crystallization within 0.5 min at a crystallization temperature of 125°C. While neat PP spent almost 3.5 min to reach crystallization completion. This indicates that the existence of CL enhances the crystallization ability of PP as well

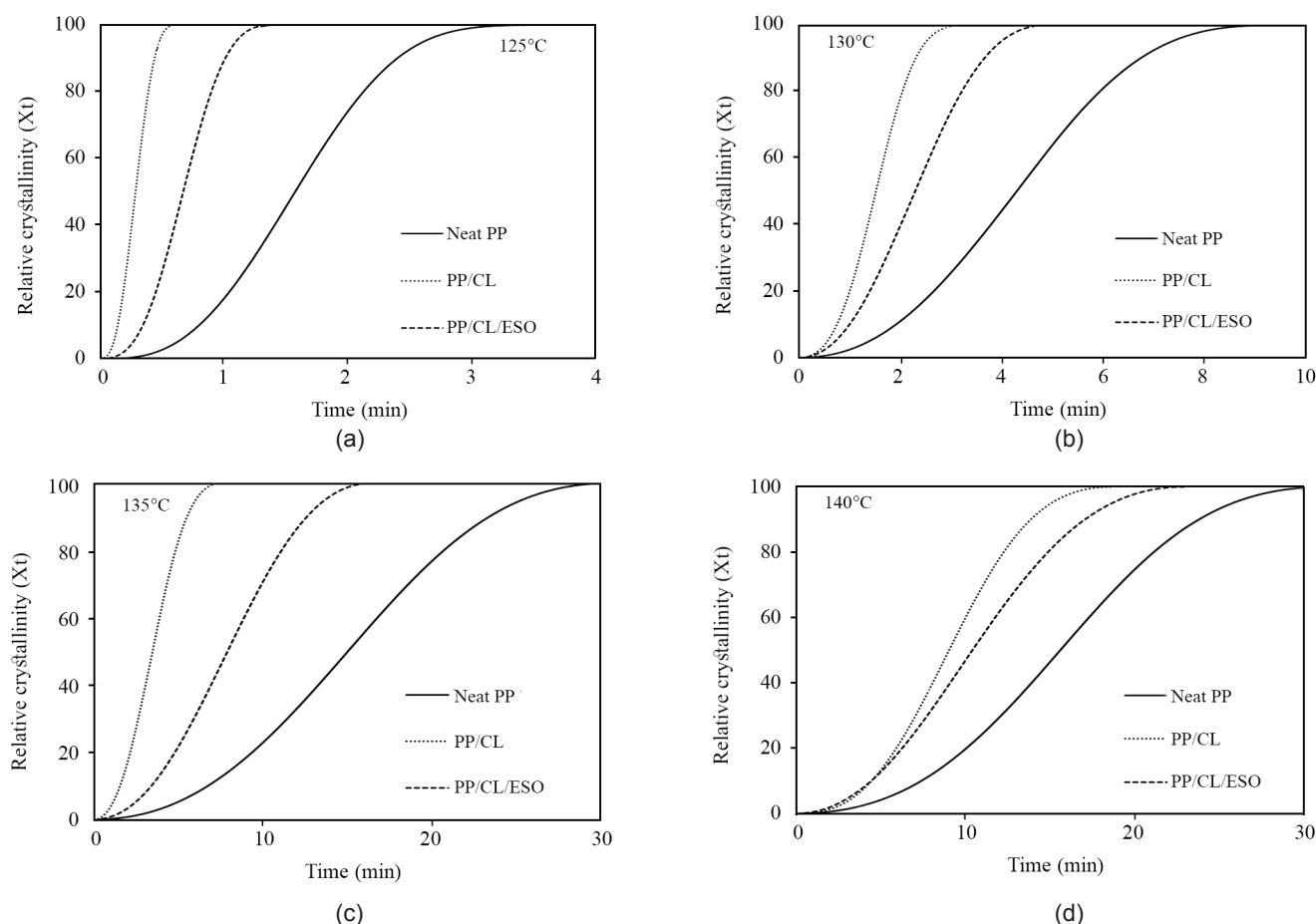


Figure 10. Relative crystallinity as a function of the crystallization time of neat PP and its composites at different isothermal crystallization temperatures of: (a) 125°C, (b) 130°C, (c) 135°C, and (d) 140°C.

as facilitates faster crystallization. In addition, the S-shape curve of PP/CL/ESO composite falls in between the neat PP and PP/CL composite, implying that ESO composite takes a longer time to complete crystallization as compared to PP/CL composite but shorter as compared to neat PP. This concludes that there may be competition among the CL and ESO to govern the crystallization of PP. Moreover, the time needed to complete the crystallization process increases with increasing the crystallization temperature.

Isothermal crystallization kinetic parameters

As is known, the crystallization of polymers consists of two stages: the primary crystallization and the secondary crystallization. Primary crystallization is the stage of the formation of a growing crystal from the molten state. Then the growth of crystal is constant at a given temperature with free growing in all directions. These circumstances are suitable to describe in more details by the Avrami equation as shown in Figure 11. Secondary crystallization is mainly related to the lamellar thickening or crystal perfection, which is

nonlinear deviation. Therefore, this later stage cannot be fitted by the Avrami equation [31-32]. Figure 11 displays the plots of $\log[-\ln(1-X_t)]$ versus $\log t$ for all samples, and the corresponding Avrami parameters are summarized in Table 2. As shown in the table, for all samples, the parameters of $t_{1/2,iso}$ increases with the increasing crystallization temperature. In other words, the higher the crystallization temperature, the slower crystallization rate, $1/t_{1/2,iso}$. This is because the thermal motion of the molecule chain is stronger at high crystallization temperatures, which limits the maintenance of the crystal lattice state [10], [33]. As compared at the same temperature, it is found that the $t_{1/2,iso}$ of all PP/CL composites is lower than those of neat PP. This result is an obvious evident to confirm that CL can act as a nucleating agent to accelerate the crystallization rate of PP. Moreover, the presence of ESO impeded the crystallization of PP/CL by showing a smaller larger $t_{1/2,iso}$ in comparison to PP/CL.

Table 2 is also contained the Avrami parameter, n , which gives information on the mechanism of nucleation and the geometry of crystal growth. The

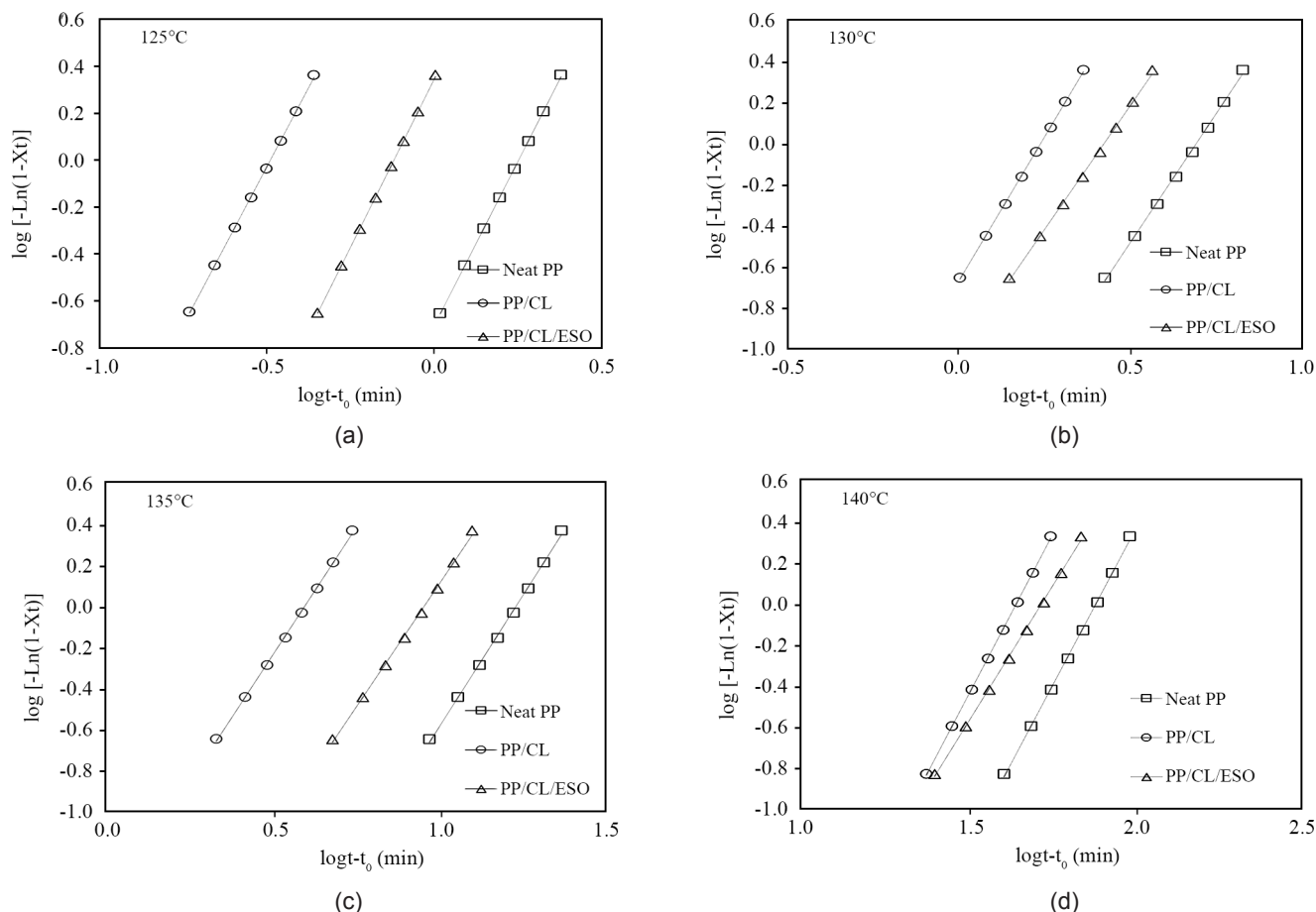


Figure 11. Avrami plots of neat PP and its composites at different isothermal crystallization temperatures of: (a) 125°C, (b) 130°C, (c) 135°C, and (d) 140°C.

Avrami parameter, n can be expressed as follows [34]:

$$n = n_{nD} + n_n$$

The n_{nD} is the dimensionality of the growing crystal. Ideally, the value of n_{nD} should be an integer between 1 and 3, corresponding one-, two-, and three-dimensional

Table 2. Avrami kinetic parameters at different crystallization temperatures.

| Samples | Temperatures (°C) | n | $t_{1/2,iso}$ (min) |
|-----------|-------------------|-----|---------------------|
| Neat PP | 125 | 2.8 | 1.6 |
| | 130 | 2.5 | 4.3 |
| | 135 | 2.5 | 15.7 |
| | 140 | 2.7 | 63.2 |
| PP/CL | 125 | 2.7 | 0.3 |
| | 130 | 2.8 | 1.5 |
| | 135 | 2.5 | 3.4 |
| | 140 | 2.7 | 37.7 |
| PP/CL/ESO | 125 | 2.9 | 0.7 |
| | 130 | 2.4 | 2.3 |
| | 135 | 2.5 | 7.9 |
| | 140 | 2.3 | 42.8 |

growth [34] time dependence of the nucleation. The n_n represents the time dependence of the nucleation. The value of n_n should be 0 or 1, where $n_n = 0$ means instantaneous nucleation, and $n_n = 1$ is the sporadic nucleation. In this present work, the nucleation can be considered as instantaneous nucleation ($n_n = 0$). As presented in Table 2, the values of n of all the samples are fraction values and varying in between 2.3 to 3.8, which is close to 3. Therefore, this can be described as a three-dimensional crystal growth [18]. However, the diffusion-controlled growth or competition for irregular boundaries of spherulites can cause the complication on crystallization [29].

CONCLUSIONS

CL and ESO were incorporated in the PP matrix and influenced the crystallization kinetics of PP. Non-isothermal and isothermal crystallizations of PP and its composites were performed. Additionally, the isothermal crystallization kinetics was investigated

using the Avrami model. From POM experiments, the spherulite size of PP became smaller, and spherulite growth was faster with the addition of CL. Compared with PP/CL, PP/CL/ESO had a large spherulite size and slower spherulite growth. The same tendency was observed in the DCS results. The DCS analyses revealed that the addition of CL provided faster crystallization and a higher crystallization rate as compared to neat PP. In addition, the containing of ESO inhibited the nucleation effect of CL. By comparing PP/CL/ESO with the PP/CL composite, it was found that the presence of ESO retarded the initiation of crystallization and decelerated the crystallization rate. However, the Avrami exponents were almost unaffected by the incorporation of both CL and ESO.

ACKNOWLEDGEMENTS

This research was funded by King Mongkut's University of Technology North Bangkok, Contract no. KMUTNB-65-BASIC-27.

CONFLICTS OF INTEREST

The authors declare that they have no conflicts of interest.

REFERENCES

1. Avalos F, Lopez-Manchado MA, Arroyo M (1998) Crystallization kinetics of polypropylene III. Ternary composites based on polypropylene/low density polyethylene blend matrices and short glass fibres. *Polymer* 39: 6173-6178
2. Gumus S, Ozkoc G, Aytac A (2012) Plasticized and unplasticized PLA/organoclay nanocomposites: short- and long-term thermal properties, morphology, and nonisothermal crystallization behavior. *J Appl Polym Sci* 123: 2837-2848
3. Al-Mulla A (2007) Isothermal crystallization kinetics of poly(ethylene Terephthalate) and poly(methyl Methacrylate) blends. *Express Polym Lett* 6: 334-444
4. Mucha M, Królikowski Z (2003) Application of DSC to study crystallization kinetics of polypropylene containing fillers. *J Therm Anal Calorim* 74: 549-557
5. Yang J, Lu S, Pan L, Luo Q, Song L, Wu L, Yu J (2017) Effect of epoxidized soybean oil grafted poly(12-hydroxy stearate) on mechanical and thermal properties of microcrystalline cellulose fibers/polypropylene composites. *Polym Bull* 74: 911-930
6. He Y, Zhou Y, Wu H, Bai Z, Chen C, Chen X, Qin S, Guo J (2020) Functionalized soybean/tung oils for combined plasticization of jute fiber-reinforced polypropylene. *Mater Chem Phys* 252: 123247
7. Pustak A, Puci I, Denac M, Švab I, Pohleven J, Musil V, Šmit I (2013) Morphology of Polypropylene/silica nano- and microcomposites. *J Appl Polym Sci* 5: 3099-3106
8. Jing Y, Nai X, Dang L, Zhu D, Wang Y, Dong Y, Li W (2018) Reinforcing polypropylene with calcium carbonate of different morphologies and polymorphs. *Sci Eng Compos Mater* 25: 745-751
9. Panda BP, Mohanty S, Nayak SK, Pandit S (2012) Fracture study of modified TiO₂ reinforced PP/EPDM composite: mechanical behavior and effect of compatibilization. *Int J Plast Technol* 16: 89-100
10. Coburn N, Douglas P, Kaya D, Gupta J, McNally T (2018) Isothermal and Non-isothermal Crystallization Kinetics of Composites of Poly(propylene) and MWCNTs. *Adv Ind Eng Polym Res* 1: 99-110
11. Bhasney SM, Kumar A, Katiyar V (2020) Microcrystalline cellulose, polylactic acid and polypropylene biocomposites and its morphological, mechanical, thermal and rheological properties. *Compos B Eng* 184: 107717
12. Alghyamah AA, Elnour AY, Shaikh H, Haider S, Poulouse AM, Al-Zahrani SM, Almasry WA, Park SY (2021) Biochar/polypropylene composites: a study on the effect of pyrolysis temperature on crystallization kinetics, crystalline structure, and thermal stability. *J King Saud Univ Sci* 33: 101409
13. Hwang TI, Kim JI, Joshi MK, Park CH, Kim CS (2019) Simultaneous regeneration of calcium lactate and cellulose into PCL nanofiber for biomedical application. *Carbohydr Polym* 212: 21-29
14. Suksut B, Khamsiang P, Sinsawat C, Kesorn N (2021) Calcium lactate as renewable filler of polypropylene: thermal, morphological and

- mechanical properties. *Suan Sunandha Sci Tech J* 8: 1-8
15. Garcia M, Vliet GV, Jain S, Schrauwen BAG, Sarkissov A, Zyl WEV, Boukamp B (2005) Polypropylene/SiO₂ nanocomposites with improved mechanical properties. *Rev Adv Mater Sci* 6: 169-175
 16. Avrami MJ (1939) Kinetics of Phase Change. I General Theory. *J Chem Phys* 7: 1103-1112
 17. Lorenzo AT, Arnal ML, Albuerne J, Müller AJ (2007) DSC isothermal polymer crystallization kinetics measurements and the use of the Avami equation to fit the data: Guidelines to avoid common problems. *Polym Test* 26: 222-231
 18. Pérez-Camargo RA, Liu GM, Wang DJ, Müller AJ (2022) Experimental and data fitting guidelines for the determination of polymer crystallization kinetics. *Chinese J Polym Sci* 40: 658-691
 19. Gopna A, Mandapati RN, Thomas SP, Rajan K, Chavali M (2019) Fourier transform infrared spectroscopy (FTIR), Raman spectroscopy and wide-angle X-ray scattering (WAXS) of polypropylene (PP)/cyclic olefin copolymer (COC) blends for qualitative and quantitative analysis. *Polym Bull* 76: 4259-4274
 20. Sedlarik V, Galya T, Emri I, Saha P (2009) Structure and conditioning effect on mechanical behavior of poly(vinyl alcohol)/calcium lactate biocomposites. *Polym Compos* 30: 1158-1165
 21. Liao N, Joshi MK, Tiwari AP, Park CH, Kim CS (2016) Fabrication, characterization and biomedical application of two-nozzle electrospun polycaprolactone/zein-calcium lactate composite nonwoven mat. *J Mech Behav Biomed Mater* 60: 312-323
 22. Yang J, Lu S, Pan L, Luo Q, Song L, Wu L, Yu J (2017) Effect of epoxidized soybean oil grafted poly(12-hydroxy stearate) on mechanical and thermal properties of microcrystalline cellulose fibers/polypropylene composites. *Polym Bull* 74: 911-930
 23. Orue A, Eceiza A, Arbelaiz A (2018) Preparation and characterization of poly(lactic acid) plasticized with vegetable oils and reinforced with sisal fibers. *Ind Crops Prod* 112: 170-180
 24. He Y, Zhou Y, Wu H, Bai Z, Chen C, Chen X, Qin S, Guo J (2020) Functionalized soybean/tung oils for combined plasticization of jute fiber-reinforced polypropylene. *Mater Chem Phys* 252: 123247
 25. Zhou H, Ye L, Li S, Li Z, Wei Z, Huang Z, Lu S, Chen D, Zhang Z, Li Y (2022) A bio-based compatibilizer (ESO-g-S-HPG) to improve the compatibility and mechanical properties of CaCO₃/HDPE composites. *Compos Sci Technol* 219: 109251
 26. Meng X, Bocharova V, Tekinalp H, Cheng S, Kisliuk A, Sokolov AP, Kunc V, Peter WH, Ozcan S (2018) Toughening of nanocellulose/PLA composites via bio-epoxy interaction: mechanistic study. *Mater Des* 139: 188-197
 27. Khare A, Mitra A, Radhakrishnan S (1996). Effect of CaCO₃ on the crystallization behaviour of polypropylene. *J Mater Sci* 31: 5691-5695
 28. Guo L, Chen F, Zhou Y, Liu X, Xu W (2015) The influence of interface and thermal conductivity of filler on the nonisothermal crystallization kinetics of polypropylene/natural protein fiber composites. *Compos B Eng* 68: 300-309
 29. Wang S, Wen B (2022) Effect of functional filler morphology on the crystallization behavior and thermal conductivity of PET resin: a comparative study of three different shapes of BN as heterogeneous nucleating agent. *Compos Sci Technol* 222: 109346
 30. Bicerano J (1998) Crystallization of polypropylene and poly(ethylene terephthalate). *J Macromol Sci Polym* 38: 391-479
 31. Keith HD, Padden FJ (1964) Spherulitic crystallization from the melt. I. fractionation and impurity segregation and their influence on crystalline morphology. *J Appl Phys* 35: 1270-1285
 32. Ravindranath K, Jog JP (1993) Polymer crystallization kinetics: Poly (ethylene terephthalate) and poly (phenylene sulfide). *J Appl Polym Sci* 49: 1395-1403
 33. Karimi S, Ghasemi I, Abbassi-Sourki F (2019) A study on the crystallization kinetics of PLLA in the presence of graphene oxide and PEG-grafted-graphene oxide: effect on the nucleation and chain mobility. *Compos B: Eng* 158: 302-310
 34. Müller AJ, Michell RM, Lozenzo AT (2016) Polymer morphology: Principles, characterization, and processing. John Wiley & Sons Inc, Ch.11, 181-203